RSC Advances

REVIEW

View Article Online
View Journal | View Issue

Cite this: *RSC Adv.*, 2020, **10**, 43640

Research progress of iron-based catalysts for selective oligomerization of ethylene

Mingzhi Wang,[a] Wei Wu,[a] Xu Wang,[b] Xing Huang,[c] Yongning Nai,[a] Xueying Wei[a] and Guoliang Mao*[a]

Received 3rd September 2020
Accepted 10th November 2020

DOI: 10.1039/d0ra07558b

rsc.li/rsc-advances

Linear α-olefins are widely used as raw materials in the chemical industry. Selective ethylene oligomerization is an important development direction of the linear α-olefin production process. Iron-based catalysts have become a research hotspot in selective ethylene oligomerization due to their advantages like high activity, high selectivity and convenience of adjusting their ligand structures. In this paper, the research progress of catalysts for selective oligomerization of ethylene was reviewed in terms of the cocatalysts, ligand structure, and immobilization of homogeneous catalysts.

1. Introduction

Linear α-olefin is an important chemical raw material that can be used to produce lubricating oil, surfactants, plasticizers and other chemical products. 1-Butene, 1-hexene and 1-octene[1–3] can be used as comonomers of ethylene in the production of linear low density polyethylene (LLDPE). The traditional α-olefin production process is a non-selective ethylene oligomerization process, and the products obtained mostly follow the Schulz–Flory distribution or Poisson distribution. The separation process with high energy consumption is required to obtain α-olefin with high purity and specific carbon number, which is difficult to meet the market demand. However, selective ethylene oligomerization can generate α-olefin with specific carbon number with high selectivity,[4–6] which can improve raw material utilization rate and reduce production cost. Therefore, this process has become an important development direction in α-olefin production. In 1987, IFP-SABIC invented an ethylene dimerization process and successfully industrialized the production of 1-butene.[7–9] In 2003, Phillips company successfully realized the industrial production of ethylene trimer for the first time, with the selectivity of 1-hexene production reaching 93%.[10,11] Sasol in South Africa achieved its ethylene tetramer production 1-octene in 2014 at the Lake Charles production site in Louisiana, USA, with capacity reaching over 100 kilotons of 1-octene and 1-hexene per year.[12–14]

Much attention has been focused on the research and development of catalysts in recent years owing to the rapid growth of the selective oligomerization of ethylene. Meanwhile, a variety of transition metal complexes (chromium, iron, zirconium, cobalt, nickel, *etc.*) are widely employed in the research of ethylene selective oligomerization. And chromium-based catalysts have attracted much researchers' interest due to their successful application in the ethylene trimerization and tetramerization production.[15–19] While discovering the excellent properties of the chromium complex, the researchers also find that other metals also perform well as active sites, especially iron,[20–22] with activity as high as 10^8 g mol^{-1} h^{-1}, even more active than metallocene catalysts. In addition, researchers could also adjust the steric hindrance by changing the ligand substituents.[23–26] In the meantime, iron-based catalysts are favored by many researchers for their advantages,[27–29] including better catalytic activity,[30–35] higher selectivity,[36–40] and good spatial variability in the spacial structure of ligands[41–44] *etc.*

The mechanism of iron-based catalysts for ethylene oligomerization can be understood as a cationic coordination polymerization process. Fig. 1 demonstrates a mechanism widely accepted by researchers in this field in recent decades,[45] and the specific steps of the process are as follows. The cocatalyst (MAO is most commonly used) first reacts with the complex, to form anion–cation pair structure through the process of ionization and alkylation. Next, the entire system undergoes ethylene monomer insertion and chain transfer at the cationic active center and the reaction mechanism of the system consists of five steps: (A) the chain growth process is represented by the coordination of ethylene with the central metal atom. And the subsequent migration of the ethylene monomer into the metal–alkyl bond is similar to the classical Cossee type[41,46,47] olefin chain growth mechanism. (B) and (C) are the transfer reactions of β-H to the metal iron atom at the active center, but there is a difference in kinetics between the two. (C) and (D) are bimolecular pathways for β-H transfer, and there is almost no difference in their kinetic behavior. (E) is the transfer process of metallic aluminum, which depends mainly on the concentration of alkyl aluminum in the reaction system, hence this kind

[a]*Provincial Key Laboratory of Oil & Gas Chemical Technology, College of Chemistry and Chemical Engineering, Northeast Petroleum University, Daqing 163318, China*
[b]*School of Foreign Languages, Anhui Jianzhu University, China*
[c]*School of Civil Engineering and Architecture, Northeast Petroleum University, China*

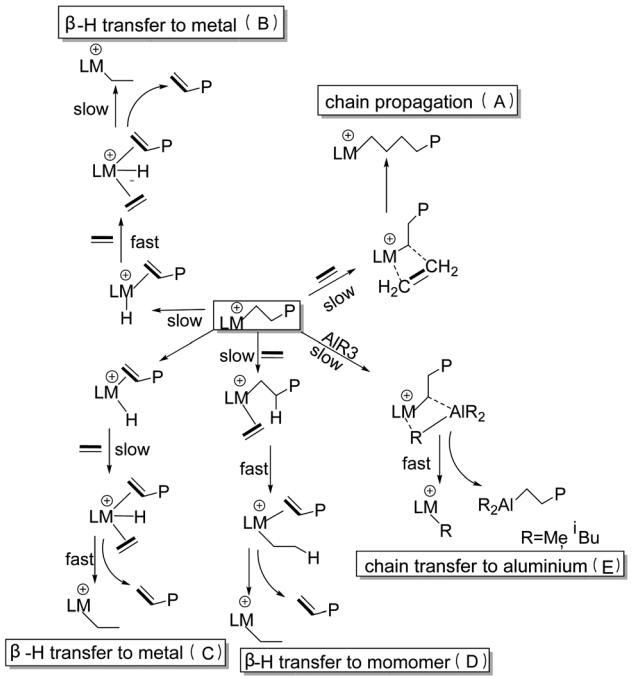

Fig. 1 Mechanism of ethylene oligomerization catalyzed by iron catalyst.

of chain transfer reaction is rare in ethylene oligomerization. Researchers (ref. 48–51) used Density Functional Theory (DFT) to calculate the energy barriers of ethylene insertion and β-H transfer of active species with different valence states. Both ferrous and ferric catalysts are used in ethylene oligomerization. However, the results showed Fe(III) as the active site is more active than Fe(II) as the active site, indicating that the valence of the active site of iron will inevitably affect the catalytic performance of the corresponding catalysts. This article gives a brief introduction to the ligand structure of the iron metal active center, the oxidation state of the active center, the loading treatment of the catalyst, and the types of co-catalysts. On top of that, some predictions involve the in-depth research in this field are also made.

2. Influence of ligand structure on the performance of iron catalyst in the ethylene selective oligomerization

In the iron-based ethylene selective catalytic system, ligands play a quite critical[45] role. Gibson and Brookhart[52,53] discovered the bisimine pyridine ligands and synthesized the corresponding complexes using Co(II) and Fe(II) as active centers respectively. It was also found that the catalytic activity of this type of catalyst was quite high, up to 10^8 g mol^{-1} h^{-1} when the iron was the metal center. Admittedly, the ligand in the catalyst system of ethylene selective oligomerization can stabilize the iron center. And the steric hindrance, substituents, functional groups, coordination angles and ligand skeletons of the ligands can directly or indirectly affect the activity or selectivity of the whole catalytic system.[54–56] Researchers found that steric hindrance and electron effects of ligands not only exert influence on the catalytic performance of the system, but also affect the distribution of products.[57–59] In recent years, the research is mainly focused on the ligands of NNN, PNN, NNO, *etc.*, among which the diimine pyridine ligands in the NNN type are most frequently (ref. 60–62) used in the iron-catalyzed ethylene oligomerization.

2.1 NNN ligand

2.1.1 Diimine pyridine type ligands. Paul J. Chirik and other researchers[63] synthesized a hetero-imine dipyridyl iron ligand and selected a PNN type ligand for comparison under the same conditions. Corresponding Fe(II) complexes (hereinafter referred to as PDI and PNN) were prepared to compare the properties of the two complexes. Fig. 2 shows the molecular structure of the two complexes. The results showed that the activity of PDI in ethylene oligomerization was much higher than that of PNN ligand. For example, when the iron source with the highest catalytic activity was selected to synthesize the corresponding complexes, the reactivity of PNN was only 1.34×10^4 g mol^{-1} h^{-1}, while the activity of complexes formed by PDI could reach 9.972×10^6 g mol^{-1} h^{-1}. As regards to the reason, it is speculated by researchers that as the amount of MAO increases, the complex PNN is more likely to generate new double PNN iron complexes with a structure similar to PNN in the alkylation process. And at the same time, the PNN complex opens the channel of the double PNN iron complex through dissociation and eventually leads to the catalyst deactivation.

WenHong Yang *et al.*[64] studied the properties of bis(imine) pyridine ligands and explored the factors affecting the thermal stability of the series ligands during ethylene oligomerization. The molecular structure of the selected ligands is shown in Fig. 3. The results show that there are three main factors influencing the thermal stability: (1) the chemical bond sequence between the active metal atoms and the nitrogen atoms in the catalyst. (2) the minimum distance between the central carbon atom and the straight chain carbon atom on the aryl group. (3) the dihedral angle of a central five-membered ring. The average experimental contributions of three factors to the thermal stability of complex **1a–1e** were 48%, 26% and 26% respectively, and the average experimental contributions to the thermal stability of complex **1f–1j** were 46%, 33% and 21% accordingly. These data indicate that the ionic bond order of the active center of ligand almost determines the thermal stability of ligand in oligomerization reaction. As for phenanthroline

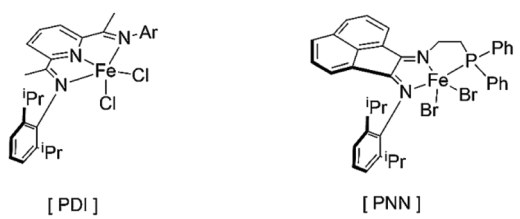

Fig. 2 Molecular structures of PDI and PNN.

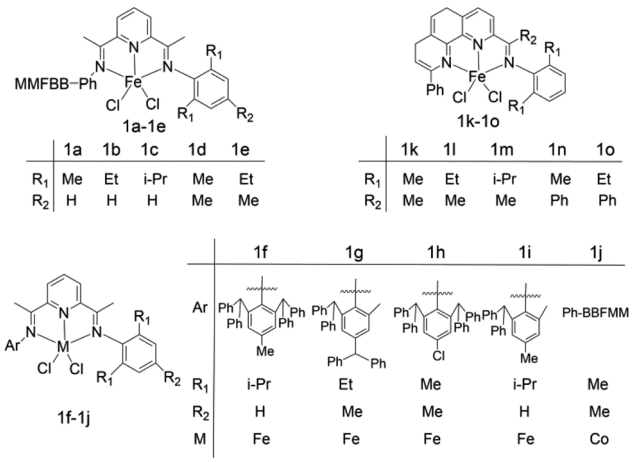

Fig. 3 Molecular structures of bis(imine)pyridine ligands.

1k–1o, dihedral angle serves as the most important role in ensuring the thermal stability of the ligand, with its contribution parameter up to 78%. The experimental data can be utilized as a molecular reference for the design of ligand with good thermal stability.

A novel multi-dentate $CyAr_2N_5$ ligand was synthesized by further derivatization of pyridine-diimine structure by Claudio Bianchini and other researchers.[65] After Fe(II) was used as the coordination center, MAO served as the cocatalyst for ethylene oligomerization. **2b** in Fig. 4 depicts the molecular structure of the new ligand. Admittedly, the ligand has better selectivity than traditional ligand **2a**. When the temperature of the system is high, the amount of oligomers produced will register a remarkable growth, and the selectivity of α-olefin will generally remain stable, approaching 100%. It was also found that the reactivity of ligands with two Fe atoms was twice or more than that of ligands with one Fe atom, and ligands with five nitrogen atoms also performed better than ligands containing only three nitrogen atoms. This is similar to Professor Sun's results.[66]

The selectivity and catalytic activity of these catalysts are very high, and it could exceed activity of metallocene catalyst when using iron as active center metal. Aside from that, this ligand also has excellent inhibition effect on polyethylene wax. By changing the steric hindrance of ligand substituents, this kind of catalyst can catalyze both ethylene oligomerization and ethylene polymerization. Furthermore, the diimine pyridine ligands are appraised as the substance of good thermal stability, and the selectivity and activity of the complexes could be changed by altering the substituents of ligands. Compared with other systems, diimine pyridine iron-based catalysts have a series of advantages, such as high activity, wide distribution and high linear selectivity, *etc.* Coupled with its relatively simple synthesis and low costs, it is actually one of the most promising catalyst for ethylene oligomerization.

2.1.2 Other NNN ligands and NN ligands. Gregory A. Solan and other researchers[67] reported a series of cycloalkyl bis(aromatic amine)pyridine ligands for ethylene oligomerization, utilizing MAO as co-catalyst. Compared with the ordinary diimine pyridine ligand, the catalyst composed of the ligands has more superior catalytic activity, selectivity and thermal stability. Fig. 5 demonstrates the molecular structure of the complex. The results showed that **3b** had the highest activity, up to 4.91×10^7 g (mol Fe)$^{-1}$ h^{-1}, and the selectivity to α-olefin was over 94%. And the main product of it was butene. The ratio of byproducts of ligand **3c** was the lowest, and the selectivity of ligand **3d** could reach over 95%. All ligands of this series showed great thermal stability. In addition, researchers found that the activity of R groups would decrease significantly when halogen elements were employed, indicating direct impacts on the activity of complexes exerted by the electron-withdrawing groups.

In 2013, Wen-Hua Sun research group[68] synthesized a series of NNN type phenanthroline ligands by fine-tuning the substituents of ligands with known structures, and coordinated it with iron. Fig. 6 shows molecular structure of various diimine dichloropyridine iron complexes. The experimental results demonstrated that both **4a–4d** exhibited high activity, among which ligand **4b** showed the highest activity (up to 4.91×10^7 g (mol Fe)$^{-1}$ h^{-1}), and the selectivity of α-olefin in the product was up to 94%. The activity of **4e–4g** is not as good as **4a–4d**, but the selectivity of 1-butene is over 90%, and there is no polymer in the product. In the comparison of ligands of **4b** series with different R_1 groups, it was found that: Br > Cl > F, thus it was inferred that the electron-withdrawing groups reduced the reactivity of ethylene oligomerization reaction. When MMAO was used as the co-catalyst, the researchers found that the activity and selectivity of the ethylene dimerization or trimerization were significantly improved due to the synthesized *o*-phenanthroline ligands. The introduction of methyl groups at the position 9 of the phenanthroline would decrease the activity of the complex while increasing the amount of α-butene, the researchers concluded.

Mingfang Zheng and other researchers[69] explored a series of *o*-phenanthroline ligands. After coordination with Fe(II) as the complex center, MAO, MMAO and $AlEt_3$ were selected as co-catalysts, and heptane or toluene was used as the solvent for ethylene oligomerization. The experimental results showed that the catalytic activity of MAO and MMAO was higher than that of

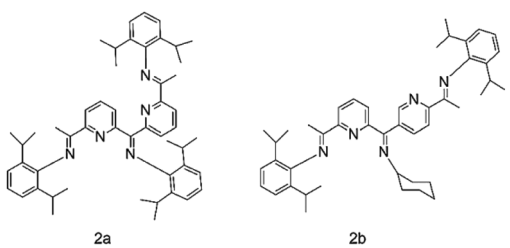

Fig. 4 Molecular structure picture of diiminopyridine type ligands $^{Ar3}N_5$ and $^{CyAr2}N_5$.

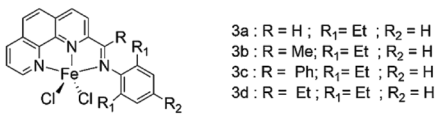

Fig. 5 Molecular structure of cycloalkyl bis(aromatic imine)pyridine complexes.

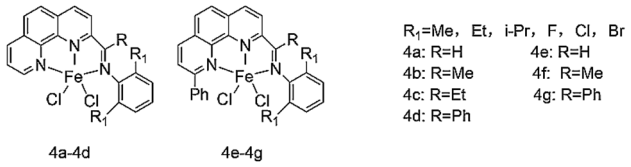

Fig. 6 Diimine dichloropyridine iron complexes.

$AlEt_3$, and $AlEt_3$ was extremely sensitive to changes in temperature and Al/Fe molar ratio. With MMAO as the co-catalyst, the best catalytic activity can be obtained when the pressure of ethylene is 1.0 MPa and the Al/Fe molar ratio is 1000, up to 3.87×10^7 g (mol Fe)$^{-1}$ h^{-1}. When MAO or MMAO is used as a co-catalyst, the selectivity of the complex for α-olefins exceeds 90%. And with the continuous increase of the aluminum–iron ratio, the selectivity of the complex for α-olefins would encounter certain fluctuations, decreasing at first and showing an upward trend gradually. In addition, the researchers found that the complex showed wonderful thermal stability throughout the process.

Researcher Pierre Alain R. Breuil[70] *et al.* reported a class of NNN ligands containing anions. Fig. 7 is the molecular structure and synthesis route of this series of NNN ligands. When Fe(III) complexes bearing the dihydro-1,10-phenanthroline ligand, MAO or TMA is utilized as cocatalyst to investigate the performance of the ligand in the ethylene oligomerization. The experimental results demonstrated that when the complex **5a** was at 80 °C, the pressure was 30 bar and the Al/Fe molar ratio was 200, the complex exhibited an activity of 2.16×10^5 g (mol Fe)$^{-1}$ h^{-1}, and good thermal stability could be found throughout the whole process. The mass fraction of butene in the oligomer was 63%, and the selectivity of 1-butene exceeded 97%. When the ratio between MAO, TMA and Fe equals 200 : 20 : 1, the mass fraction of butene in the oligomer products could reach 66%, and the selectivity of 1-butene is over 98% despite a slight decrease in reactivity. Under the same conditions, the complex **5b** with the metal active center as Fe(II), the complex **5c** with three chlorine substituents attached to the active center, and the deprotonated complex **5b–5d** participated in the oligomerization of ethylene respectively. The results did not show any reaction activity and selectivity. Based on this, it could be drawn that the oxidation state of the ligand-linked anion donor and the metal active center of the complex is a key factor affecting the activity and selectivity of the catalyst.

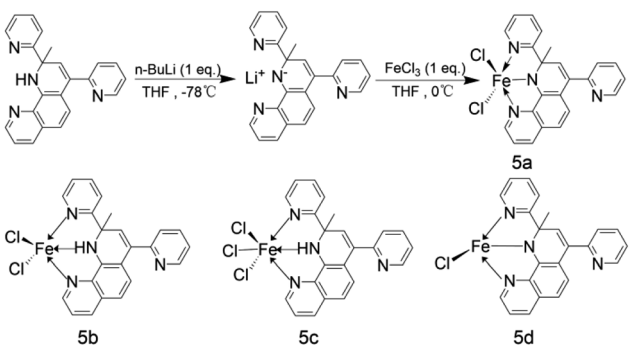

Fig. 7 Molecular structure of tridentate N,N,N-type iron catalysts.

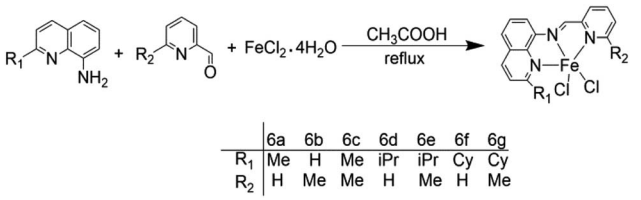

Fig. 8 Synthesis route of quinolines derivative tridentate metal complexs.

Wen-Hua Sun and other coworkers[71] synthesized a series of tridentate ligands of *N*-(pyridin-2-acyl)-quinolin-8-amine derivatives, and MAO and MMAO as co-catalysts to carry out ethylene oligomerization. Fig. 8 shows the structure of the complexes. It has been found that the volume of substituents can affect catalytic activity of the complex. When the co-catalyst is MMAO, its catalytic activity ranges from 1.0×10^5 g mol^{-1} (M) h^{-1} to 1.0×10^6 g mol^{-1} (M) h^{-1}. With MMAO as a co-catalyst, the highest activity of **6e** can reach 2.77×10^6 g mol^{-1} (Fe) h^{-1}. The proportion of C_6 components can be increased by increasing temperature or decreasing pressure appropriately. The activity of the **6g** with the largest substituent volume is the highest, up to 2.83×10^6 g (mol Fe)$^{-1}$ h^{-1}. The researchers then speculated that the catalytic activity of the ligand will be improved when the active center is protected by large steric hindrance or a large number of substituents. When R_1 or R_2 is attached to a large substituent, the selectivity of 1-butene will be higher than 90%.

Subsequently, researchers[71] developed a class of bidentate NN and tridentate NNN ligands **7a–7d**, and selected Et_2AlCl, MMAO, MAO, *etc.* as co-catalysts to explore the actual effects of the ligands in ethylene oligomerization reaction. The molecular structure of the ligand is shown in Fig. 9. After experiments, it was found that when the ligand was treated with MAO, its catalytic activity was as high as 1.43×10^7 g (mol Fe)$^{-1}$ h^{-1} with the α-olefin (C_4–C_{28}) being produced, and the selectivity exceeded 99%. Under the same conditions in other experiments, Et_2AlCl was found to the best results. Their oligomerization activity varies with R group on the complex. The order of activity was Me < Et < i-Pr, and the order of activity of substituents corresponding to halogen groups was Cl < Br. The explanation given by researchers was that the larger group had a protective effect on the active metal center, thus increasing the activity of the corresponding catalyst. The oligomerization products obtained after reaction basically accord with Schulz–Flory distribution. And the synthesis method of the ligand is rather simple.

Most NNN ligands have quite high activity and selectivity, accompanied by fabulous thermal stability. The selectivity and

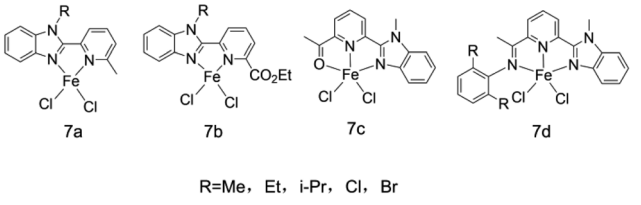

Fig. 9 Molecular structure of bidentate type NN ligands and tridentate type NNN ligand.

activity of the ligands demonstrate significant rise when the ligands are connected with substituents with large steric hindrance or great amount. The electron-giving groups attached to the ligands can improve the activity of the complexes, and the Al/Fe molar ratio also has essential impacts on the selectivity of the reaction product. The performance of the NN ligand is similar to that of NNN ligand, but the catalytic activity and selectivity do not demonstrate the same excellence as the NNN.

2.2 PNN ligand

Stephen O. Ojwach and other researchers[72] synthesized two diphenylphosphoryl pyridine ligands **8a** and **8b**, and conducted ethylene oligomerization under the same conditions with MAO or $AlMe_3$ as co-catalyst and benzene as solvent. Fig. 10 shows the synthesis route of pyrazoline phosphopyridine ligand. According to experimental results, the main product of the catalytic system was C_4 component, and its selectivity was up to 99%. During the study, it was also found that the catalytic activity of the catalytic system would plunge when the substituent on the pyridine ring was replaced by a larger group. It was attributed to the fact that the larger group prevented the ethylene monomer from contacting the active center of the metal. Moreover, the researchers found that the selectivity of α-C_4 decreased over time, which might be caused by increased α-C_4 isomerization that resulted in 2-butene formation. When the pressure in the experimental system increased from 10 bar to 30 bar, the catalytic activity also increased from 3.6×10^5 g (mol Fe)$^{-1}$ h^{-1} to 4.30×10^5 g (mol Fe)$^{-1}$ h^{-1}, and the selectivity of α-C_4 rose from 65% to 77%. The researchers later suggested that the increased dimerization rate may limit the parallel isomerization of 1-butene to 2-butene.

The PNN ligand has extremely high selectivity and activity, and such properties of its corresponding complex can be easily changed by controlling the pressure of the system. The solvent benzene matched by the ligand, nevertheless, will exert harmful impacts on the environment. So we are waiting for us to explore or find a better solvent.

2.3 NNOO ligands

Cui-Qing Li and other coworkers[73] synthesized a class of hyperbranched salicylaldehyde ligands and used Et_2AlCl and MAO as co-catalysts for ethylene oligomerization. Fig. 11 shows the synthesis route of the complex. The reaction activity and product selectivity of ethylene oligomerization can be easily controlled by changing the reaction temperature, pressure and the Al/Fe molar ratio. The reactivity of these complexes decreases with the increase of alkyl chain length. After activation with MAO, the catalytic activity of the complex could reach 8.17×10^4 g (mol Fe)$^{-1}$ h^{-1}. When $EtAlCl_2$ was used as co-catalyst, the catalytic activity could be up to 1.102×10^5 g (mol Fe)$^{-1}$ h^{-1}. Then the researchers tested the catalyst with different solvents. When toluene was used as the solvent, the main product was found to be butene (62.64%); when cyclohexane was used as the solvent, the main product was longer-chain oligomers with a content of 53.01%. When the solvent was hexane, the main product was hexene with a content of 73.74%. The researchers speculated that the increased catalytic activity of the catalyst may accelerate the chain termination reaction. It was also found that the higher the proportion of low-carbon components makes up in the product, the faster the chain ends. The product of ethylene oligomerization is also affected by solvents, that is similar to Yankey's results.[74]

Jun Wang and other researchers[75] also developed a new hyperbranched salicylaldehyde diamine ligand. Fig. 12 shows the synthesis route of the complex. It was found that compared with the absorption peaks of free ligand, the electronic absorption peaks of the complexes **10a–10d** were red-shifted at 234 nm, 259 nm and 322 nm, and at the same time the n→π* absorption intensity of the C=N bond weakened. It is thus speculated that coordination effect between Fe and N atoms does exist, so that the catalytic activities of complexes **10a–10d** are not as high as expected, contrary to the higher selectivity of high carbon olefins (C_{10} and higher carbon number olefin); solvents have direct impacts on the activity of the complexes. When toluene is used as the solvent, the activity of the complex **10a–10d** is significantly higher than the complex where the methylcyclohexane is used as the solvent. As a matter fact, the great polarity of the solvent has increased the ethylene insertion rate and the solubility of the complex, so the catalytic activity will rise accordingly. At the same time, the selectivity of the complex is largely influenced by the solvents. When other conditions remain unchanged, the selectivity of complex **10a** for

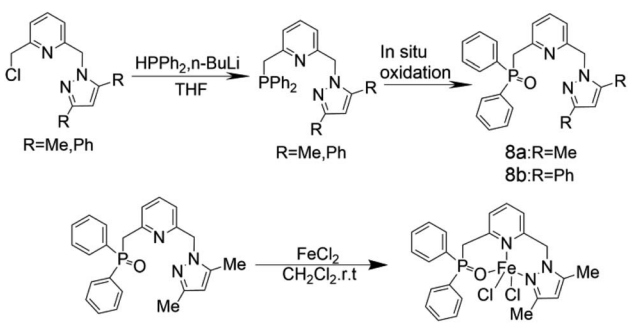

Fig. 10 The reaction process of pyrazoline ligands to generate corresponding complexes.

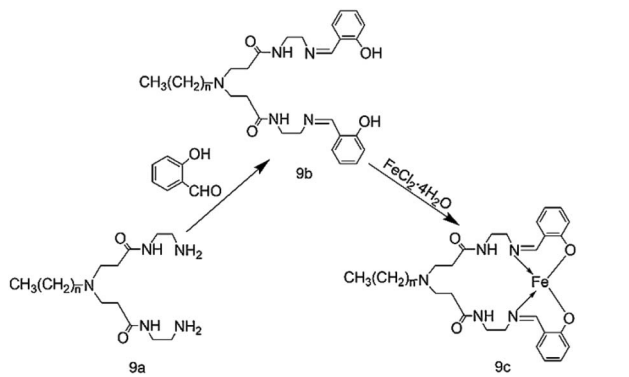

Fig. 11 Synthesis route of the hyperbranched salicylaldehyde diamine.

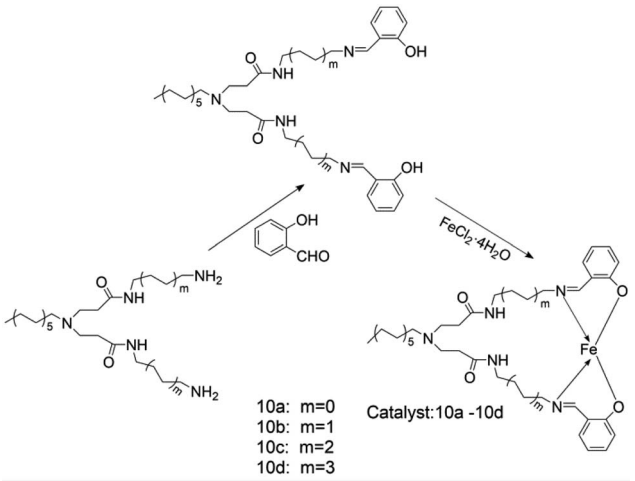

Fig. 12 Synthesis process of the new hyperbranched salicylaldehyde diamine metal complex.

higher olefins increases from 1.16% to 20.48%, and the selectivity of complex **10c** rises from 1.96% to 15.89% when using toluene instead of the original solvent methylcyclohexane. It indicates that the environment of metal active center has actually direct affects on the oligomerization of chain and chain transfer process. The researchers also found that the selection of different co-catalysts also has great influence on the activity and selectivity of the complex. For all iron(II) complexes **10a–10d** activated with MAO, the catalytic activities were much lower, attaining from 2.62×10^4 g mol^{-1} h^{-1} to 6.94×10^4 g mol^{-1} h^{-1}. Activation of iron(II) complexes **10a–10d** with DEAC instead of MAO produced in general much more active systems (catalytic activities varying from 4.70×10^4–8.17×10^4 g mol^{-1} h^{-1}),but the selectivity of the high carbon olefins decreased to about half of the original selectivity. Such ligands have high selectivity to high-carbon number olefins and do not require MAO catalysis, which greatly reduces the experimental cost.

Azadeh Tadjarodi and other coworkers[76] synthesized a series of 2-(1-*H* benzimidazole-2-acyl)-phenol ligands and conducted ethylene oligomerization employing Et_2AlCl as co-catalyst. Fig. 13 shows the molecular structure of the phenol ligand skeleton and various electron-absorbing groups attached. It was found that the groups attached to the ligand directly affected the effect of the catalyst. In all such complexes, the ligands were coordinated as bidentate, *via* the C=N nitrogen atom and a phenol oxygen atom. In addition, among all the divalent iron complexes, the complexes with four unpaired electrons have the lowest structural energy, indicating that the complexes are basically in a high spin mode. The researchers found that the complex has a good selectivity for 1-butene under the pressure of 2.0265 MPa. The experimental effect of co-catalyst using Et_2AlCl is better, and the catalytic activity can reach 1.686×10^6 g mol^{-1} h^{-1}. A noticeable phenomenon was also spotted by researchers that there is no oligomerization product containing odd carbons in the product. According to the research data, **11a** ($R_1 = R_2 = H$) has the worst catalytic activity, and **11d** ($R_1 = R_2 =$ Cl) performs best. The catalytic activity of these five complexes is ranked as follows by a large number of experiments: **11d** > **11b** > **11c** > **11e** > **11a**. By comparison, it was found that the electron-absorbing groups attached to the ligands could improve the catalytic activity of the complexes. In this regard, the researchers concluded that the attachment of electron-absorbing substituents on the ligands (with appropriate reduction in the electron density of the active metal center) is more conducive to the combination of ethylene with the active metal center, thus achieving better catalytic activity.

Compared with other types of ligands, NNOO ligands have brilliant selectivity for high-carbon alkenes. The solvent toluene, nevertheless, which is the best match of the ligands, might not be environmentally friendly, and a better solvent replacement is waiting to be found. Moreover, the reactivity of the complex plunges with the increase of alkyl chain length. And the activity and selectivity of the catalyst parameters corresponding to the ligand could be easily controlled. What's more, some NNOO ligands attached with electron-absorbing groups can improve the catalytic activity of the complexes, which was opposite to the NNN ligand.

2.4 NNO ligand and NO ligand

Ying Zhang and other researchers[77] synthesized two types of NO-type multi-site pyridine ligands **12a** and **12b**, both of which were coordinated with Fe(III) as the metal active center, and Et_2AlCl was used as a co-catalyst to carry out ethylene oligomerization. Fig. 14 shows the molecular structure of two metal complexes. Researchers found that when the system pressure of **12a** increased from 0.6 MPa to 1 MPa, the catalytic activity of the complex rose from 0.79×10^5 g (mol h)$^{-1}$ to 1.48×10^5 g (mol h)$^{-1}$, and the yield of C_4 products also grew from 67.16% to 90.41%. The research results showed that properly increasing the pressure of the system is better for the coordination of ethylene and active sites, and it can effectively suppress the chain growth, thereby increasing the content of 1-butene. When Al/Fe molar ratio equals 500, the maximum catalytic activity is 1.48×10^5 g (mol h)$^{-1}$. And **12b** is, in fact, inferior to **12a** in all aspects. Researchers believe that sufficient amount of Et_2AlCl is needed to maintain the high activity of the reaction. However,

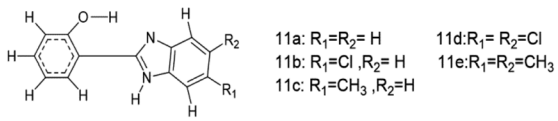

Fig. 13 Molecular structure of phenol ligands.

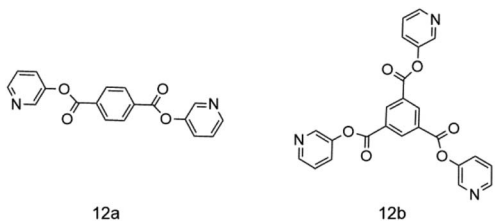

Fig. 14 Molecular structure of multi-site pyridines.

excessive amount of Et_2AlCl will lead to more aluminum impurities, which may cover the active site and greatly affect the catalytic effect. Moreover, the selectivity of butene in the oligomerization products is significantly improved in that Et_2AlCl inhibits the chain growth. The high catalytic selectivity is attributed to the regular structure and low metal steric resistance.

Hideki kurokawa and other experts[78] explored a new acetimide pyridine ligand coordinated to iron metal, using triethyl aluminum or triisobutyl aluminum as a co-catalyst to conduct ethylene oligomerization. Fig. 15 shows the synthetic route for the preparation of the catalyst. The experimental results presented that the final products of **13a** complex involved in ethylene oligomerization were almost all polymers. However, the selectivity of **13b** complexes to α-olefin was over 95%, and the oligomerization products met the Schulz–Flory distribution. Aside from that, complexes **13c** and **13d** also demonstrated some activity for ethylene oligomerization, yet it is much lower than that of **13b**. The results showed that if the positions of the same group of substituents on the ligands are exchanged, the selectivity and activity of the complexes may also be greatly affected. In the meantime, the researchers found that TiBA was more effective as a cocatalyst than MAO. In addition, the complex can be loaded with a specified carrier, and after the reaction, the complex can be separated from the oligomer through filtration. Actually the ligand has demonstrated long life and high activity.

Under suitable conditions, NNO ligands could exhibit high activity and selectivity, and non-aluminoxane can be used as co-catalyst for decreasing costs. The NO ligand is actually equipped with great selectivity and activity. And the selectivity can be controlled by changing the pressure of the system, while the amount of co-catalyst should be strictly controlled in the ethylene oligomerization process.

3. Effect of cocatalyst on the performance of iron-catalyzed ethylene selective oligomerization system

The competitive reaction between the chain growth and the β-H chain transfer in the process of ethylene oligomerization catalyzed by iron catalysts is the dominant factor affecting the distribution of ethylene oligomerization products. And the process of ionization and alkylation of active center by co-catalyst directly affects the competitive reaction. In order to solve these two problems, developing a new co-catalyst to enhance the β-H transfer reaction by regulating its interaction with the active center is rather helpful, thus reducing the proportion of polyethylene wax as a by-product.[44] There are several ways for cocatalysts to make transition metal centers active including group alkylation transfer,[79–82] deprotonation,[83–86] cationization[87] and ligand semi-coordination[88] *etc.* The nature of the oligomerization of ethylene catalyzed by iron-based catalysts is the coordination polymerization of the cationic active center. The main function of the cocatalyst is to provide sufficient alkyl to provide sufficient alkyl to the active center for alkylation. After the alkylation, the cocatalyst body will also take the electron-rich group into a balanced anion and form a dynamic equilibrium with the cation center. It is in this dynamic equilibrium that the active center can selectively complete the ethylene insertion and chain transfer processes.[89] Based on the current research and the ring mechanism of mononuclear Fe metal in ethylene oligomerization, the valence state of iron elements is divalent and trivalent, *etc.* Combined with previous literature, it can be concluded that the application of co-catalysts in the whole catalytic process is mainly manifested in the following aspects:[90] (1) the co-catalyst acts on the iron metal center and produces an alkylation effect, thereby achieving the catalytic effect.[91,92] (2) The co-catalyst separates the alkylation groups on the metal center so that ethylene has more opportunities to contact with the metal active center, greatly increasing the reaction frequency of ethylene monomer and the metal active center.[93] (3) Part of the co-catalyst interacts with the center of the iron metal to produce anion–cation pairs, thereby enhancing the catalytic effect of the catalyst.[94]

Yongrong Yang and other coworkers[95] studied the effect of iron complexes with diimine pyridine ligands in catalytic ethylene oligomerization utilizing aluminoxane series compounds, such as modified methylaluminoxane (MMAO), commercial methylaluminoxane (MAO-C) and synthetic methylaluminoxane (MAO-S) as co-catalysts. When the co-catalyst EAO (ethyl aluminoxane) was selected, the activity of the catalyst decreased significantly due to β-agostic[96] effect. In the meantime, the selectivity of the product increased drastically and the proportion of olefin in the by-product reduced. Referring to MAO-C, MAO-S showed higher catalytic activity, but the proportion of by-products was also great. The catalytic activity of MAO-S was much higher than that of MAO-C (the highest activity of MAO-S could reach 1.305×10^7 g mol^{-1} h^{-1}), which might be caused by partial component decomposition or the incomplete formation of the active part of methylaluminoxane during the reaction. The researchers also utilized MBAO (mixed aluminoxane) and EAO (ethyl aluminoxane), both of which showed brilliant performance. Compared with the above catalysts, i-BAO can not only improve the selectivity and reduce the proportion of by-products, but also help to extend the life of the catalyst. Therefore, i-BAO is considered to be the co-catalyst with the best comprehensive performance, with the best catalytic effect under the condition of $H_2O/Al = 0.7$. The researchers also found that the introduction of isobutyl groups in iron-based catalysts was conducive to delaying the chain transfer process and reducing the proportion of polyethylene as a by-

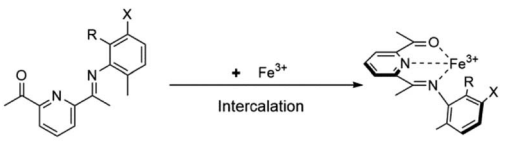

13a: R=CH_3 , X=H ;
13b: R=H , X=CH_3 ;
13c: R=H , X=H ;
13d: R=H , X=Cl ;

Fig. 15 Molecular structure picture of acetylenimine pyridine ligands.

product. Meanwhile, the introduction of large groups of phenolic compounds or siloxanes can reduce the proportion of polymers (by-products) during ethylene oligomerization and help promote the rate of transfer of β-H.

Tongling Li and other coworkers[97] synthesized a class of *o*-diazophene ligands and studied the effects of different co-catalysts on the oligomerization activity and selectivity of ethylene. The researchers found that compared with the modern water-free catalyst system, the system could obtain higher oligomerization activity (the activity of the water-bearing system was about 10 times that of the water-free system under the same conditions). Meanwhile, the system could also rapidly initiate the reaction with good stability and repeatability. When triethyl aluminum (TEA) was used as co-catalyst and toluene as solvent, the proportion of α-olefin in the product reached 97.8%, and the catalytic activity was 5.1×10^6 g (mol Fe)$^{-1}$ h^{-1}. Then the researchers conducted ethylene oligomerization with triisobutyl aluminum TIBA and triisopropyl aluminum TIPA as co-catalysts and found high selectivity, and the ethylene oligomerization activity approaches or exceeds 1×10^7 g mol^{-1} h^{-1}. It is believed that TEA boasts better reducing power than TIBA and TIPA, thus exhibiting relatively better performance.

Pierre Braunstein[98] synthesized Fe-type self-activated mixed valence ethylene oligomerization catalyst by using NPN ligand with CH_2Cl_2 as solvent. Fig. 16 shows the synthesis process of three such catalysts. When MAO or $AlEtCl_2$ was used as the cocatalyst, the iron-based catalyst showed moderate activity in the oligomerization reaction and only a small amount of 1-butene was produced. It is believed that the ligand has low steric hindrance, which reduces the molecular weight of ethylene oligomer.

The co-catalysts commonly used in ethylene oligomerization are MAO[45,99–102] and MMAO,[103,104] while their high cost restricts the industrial application of the co-catalyst in the selective oligomerization of ethylene.[105–109] Therefore, finding a new co-catalyst that can replace MAO has become one of the hot issues in this field.[110–115]

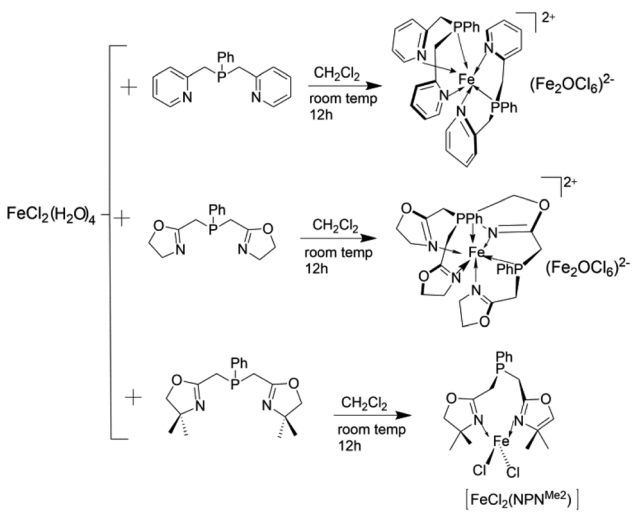

Fig. 16 Synthesis steps of NPN type iron system self-activated mixed valence catalysts.

Theodorus de Bruin and other researchers[116] used a dimer aluminum complex $[PhOAlMe_2]_2$ with known specific structure as co-catalyst to participate in the ethylene oligomerization reaction and used({2,6-(2-$(CH_3)C_6H_4N{=}C(CH_3))_2$–$C_5H_3N$}Fe(II)$Cl_2$) (abbreviated as [LFe(II)Cl_2]) as the catalyst precursor. The experimental results showed that the co-catalyst could activate [LFe(II)Cl_2] and generate a cationic iron alkylation [LFe(II)Me]$^+$, while the co-catalyst itself generated a chlorinated anion, which could improve the catalytic activity of the ligand. What's more, the researchers found that the cocatalyst should not contain (or be easily produced in the reaction) trivalent aluminium sites, as this may result in the formation of cation addendum which would greatly reduce the activity of the catalyst.

In this regard, Pierre Alain R. Breuil and other coworkers[117] were eager to find out an aluminum-based co-catalyst that could be used for ethylene oligomerization of iron catalyst, so they used a series of hydroxyl compounds to react with trimethyl aluminum to prepare a new type of co-catalyst, **14a** and **14b**. The experimental results showed that the catalytic reactivity could reach 9.3×10^5 g (mol Fe)$^{-1}$ h^{-1}, but obtaining a Schulz–Flory distribution of oligomers with K equaling 0.70 was an undoubted deficiency, and actually no solid polymers were found. Fig. 17 shows the molecular structure of the co-catalyst replacing MAO. The experimental results showed that the activity of this series of co-catalysts is lower than that of MAO, but they can activate the iron complexes in the system and have the very potential to become a new generation of co-catalysts. The next goal of the researchers is to explore the role of each aluminum atom in the aluminum cocatalyst **14a** and **14b** in the activation process.

Jian ye and other researchers[118] synthesized a class of bis(imine)pyridine ligands (BIP) and utilized MAO as co-catalyst to investigate the effects of cocatalyst in ethylene oligomerization by adding phenols, ether carboxylic acids and other oxygens. The results showed that phenoxy group could directly affect the proportion of polymer in the product. Phenoxy group in the complex can greatly reduce the molecular weight of the product and delay the formation of polymer. The amount of insoluble polymer in the product decreased from 31.9% to 5.5% while the production of α-olefin could always maintain at a high level when the ratio of phenol to MAO increased from 0 to 0.7. The researchers also found that when phenoxy ethylene group was found in the system, the cation active electron pair could be better separated, which was beneficial to further reduce the proportion of by-products. For example , when the molar ratio of 2-NaPhOH/Al increases from 0 to 0.7, the mass fraction of insoluble polymer plunges while the mass fraction of C_4–C_{12}

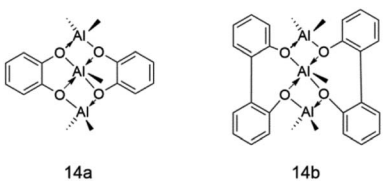

Fig. 17 Molecular structure picture of a new type of aluminum catalyst promoters.

olefins registers a remarkable growth. When the ratio is 0.3, the mass fraction of insoluble polymer is as low as 1%. Therefore, it can be inferred that 2-NaPhOH can effectively reduce the relative rate of chain propagation to chain termination. It can also be concluded that phenolic compounds with larger aromatic rings have stronger polymerization resistance. When PhOH and 1-NaPhOH were taken as experimental subjects, it was found that the activity of the complex is relatively high when PhOH/Al = 0.7, while activity of the complex could be high for 1-NaPhOH under the circumstance of 1-NaPhOH/Al = 0.3. Based on these, it can be concluded that with the increase of acidity of phenolic modifiers, the deactivation probability of catalytic system can be greatly reduced.

4. Loading of iron-catalyzed system in ethylene selective oligomerization

Homogeneous iron-based catalysts have the advantages of high activity[119,120] and selectivity.[121] Furthermore, structural alterations of complexes[70,71,77–89] can be easily made. However, iron complexes are sensitive to temperature, so the catalytic time of iron complexes in oligomerization reaction is relatively short.[77,93] Juan Cámpora and other coworkers[122] found that the environment around the active center had significant influences on ligands in iron complexes. These influencing factors involve not only temperature, but also reaction pressure and types of co-catalysts *etc.* Therefore, it is suggested to support the catalyst to improve the stability of the reaction. Other experiments showed that the diffusion effect of the monomer is directly influenced by the pore channels of the molecular sieve. Therefore, the catalytic activity of catalysts in olefin polymerization is slightly decreased compared with that in homogeneous catalysis. Nevertheless, the chain termination and chain transfer reactions of the catalysts are both effectively inhibited. Based on a large number of experimental studies, it indicates that the experimental effect of the catalyst supported by the carrier in the process of ethylene oligomerization is mainly affected by three factors including temperature,[123–126] concentration[127,128] and the pore diameter of the carrier.[129–131]

In the polymerization reaction or oligomerization reaction of olefin, catalysts are supported in two main ways. The first, catalysts are directly supported on the carrier. The second is to modify the carrier with alkyl aluminum or alkyl-aluminoxane before loading. The latter loading method can better control the structure of the polymer and reduce the deactivation of the active center. And employing such way of loading during polymerization can choose cocatalyst for research. For instance, polymerization reactions of such kinds of carriers including SBA-15,[132–134] MCM-41,[135–137] NaY[138–140] and ZMS-5 (ref. 141 and 142) molecular sieve. In the regard, MAO or TEA are the most commonly used cocatalyst.

Dimerization of ethylene over iron-based catalysts supported on a class of metal–organic frameworks (MOF) has been reported by Jerome Canivet and other researchers.[143] The experimental results indicated that the proportion of C_4 components in ethylene oligomerization products with 10Ni@(Fe)MIL-101 supported system under the condition of heptane as solvent, Et_2AlCl as co-catalyst and system pressure of 15 bar was as high as 95%, and the catalytic activity of olefin was 1.0455×10^4 g mol^{-1} h^{-1}. However, the selectivity of α-olefin applying homogeneous catalytic system was dramatically reduced. The change in the behavior of the catalytic system indicates that the supported material can promote the elimination of β-H and thus generate short chain α-olefin more easily, thereby improving the selectivity of ethylene dimerization. The carrier not only ensures the high surface active site density, but also isolates single active site, avoiding the loss of activity caused by the contact between active sites, and in such way the activity of the catalyst can be significantly enhanced. The researchers also found that the MOF system is reusable, inexpensive, and environmentally friendly. Han Yang *et al.*[91] also investigated a new type of organometallic framework and supported iron-based catalysts on the carrier material to catalyze ethylene oligomerization. The results demonstrated that the main factors affecting the catalytic activity of MIL-100(Fe) supported catalyst system are as follows: (i) the surface area of the catalyst system; (ii) the content of the unsaturated site of Fe. The selectivity for octene was over 80%, but the researchers found that the high selectivity of the supported catalyst could not be attributed to the steric hindrance of the pore structure of MIL-100(Fe), but to the properties of the metal site itself. It has also been found that temperature can directly affect the loading effect of the carrier by changing the pore size, thereby indirectly affecting the activity of the catalytic system. For example, the activity of the catalytic system is on the rise in the range of 150 °C to 250 °C. When the temperature is higher than 250 °C, the catalytic activity shows a downward trend.

Cun-Yue Gao *et al.*[144] reported a series of MMS mesoporous molecular sieve carriers with ordered mesoporous structure, uniform and adjustable pore size and stable skeleton structure. Moreover, the inactivation of active sites could be effectively inhibited. The pore size of molecular sieve determines the influence of temperature and pressure on the activity of the catalyst system. The larger or smaller pore size of molecular sieve support will greatly reduce the activity of the supported catalyst. It was also found that with the increase of Al/Fe molar ratio, the activity of the supported catalyst increased at first and decreased gradually, while the product distribution remained steady. What's more, the type of active site formed during polymerization of the catalyst linked to the carrier is also related to the concentration of ethylene and the pore size of the carrier. The mesoporous carriers which exhibit high activity during ethylene oligomerization include SBA-15, ITQ-2, MCM-22, *etc.*

The immobilization of iron-based catalysts on mesoporous molecular sieves and their catalytic performance in ethylene oligomerization were also reported by Qingyuan Guo and other coworkers.[135] The diimine pyridine iron complex was supported on SBA-15 and MCM-41 respectively, and activated with MAO. The results indicated that the ethylene oligomerization ability is greatly affected by the pore size of the carrier and the temperature of the system. The catalytic activity of MCM-41 for low-carbon olefins is higher than that of SBA-15. The possible reasons are as follows: (i) the thermal stability of MCM-41 is much better than that of SBA-15 in oligomerization; (ii) there

might be synergistic effect between molecular sieves and complex; (iii) temperature rise speeds up chain propagation as it is, chain transfer, particularly β-H elimination, quickens faster than chain propagation, thus forming more low molecular weight oligomers. In terms of reaction temperature, the researchers believe that the diffusion effect caused by the carrier inhibits the activity of the catalyst and the rate of ethylene monomer reaching the active metal site when the reaction temperature is low. When the temperature is high, the activity of the corresponding homogeneous complex decreases rapidly or even deactivates while the supported complex remains unchanged, which indicates that the carrier material can effectively improve the thermal stability of the complex. It was also found that the distribution of the products in the loaded catalytic system was almost unaffected by the aluminum-iron ratio, suggesting that β-H transfer was the dominant reaction for chain transfer and the transfer to Al, from activator, is insignificant.

On the basis of a large number of published experimental results, it can be concluded that the overall catalytic activity of non-supported catalysts is much higher than that of supported catalysts. The supported catalysts, however, has the following advantages:(i) the reactants are well immobilized by the carrier material, which greatly improves the thermal stability of the reaction; (ii) the pore channels of molecular sieves are not only the carrier of catalysts, but also the reactor of ethylene oligomerization, enabling efficient catalyst immobilization and control of the polymerization reaction; (iii) nano-pore has stereoselectivity effects on monomer insertion and polymerization, which is beneficial to increasing the selectivity of α-olefin. In terms of catalyst selectivity, both supported and unsupported catalysts demonstrated brilliant performance. As far as the effect of catalytic reaction is concerned, the activity of the unsupported catalyst can reach the maximum soon, but it could only maintain for a short time. And admittedly the decline rate is rather higher after its peak. The performance of the supported catalyst is quite different from that of the non-supported catalyst. To be more specific, it actually takes a long time for the supported catalyst to reach its maximum while being able to last for a long time. Moreover, the degradation rate of catalytic activity is quite slow after reaching the maximum.

5. Summary and prospect

Recent studies have shown that the diimine pyridine ligands in the ligand series selected for iron-based catalysts have higher activity,[145–150], (with MAO as co-catalyst and the addition of proper amount of specially treated phenolic compounds, the maximum catalytic activity can exceed 1.0×10^8 g mol^{-1} h^{-1}). Furthermore, if the ligands of the series are connected with small groups, then the selectivity of the target products can be improved. Aside from that, the coordination structure of the aluminum atom in the cocatalyst and the electronic environment play actually essential role in inhibiting the reaction of polyethylene wax in the product. Admittedly, the interaction between the anion–cation pairs will be stronger after alkyl exchange by increasing the density of the electron cloud around the aluminum atoms and decreasing the ability of the aluminum atoms to disperse electrons. Despite the fact that the insertion growth of ethylene slows down and the activity decreases in this way, the transfer reaction of β-H chain will be obviously enhanced, which could inhibit the production of polyethylene wax. The effect of TMA is rather nice in non-aluminoxanes co-catalysts, and is no worse than MAO. The thermal stability of supported catalysts composed of MCM-41 and ZSM-5 with corresponding complexes is better than that of homogeneous catalysts. The ratio of low carbon number olefins in the products of supported catalysts is higher than that of homogeneous catalysts due to the type selection effect of the internal channels of molecular sieves, therefore, the ratio of low carbon number olefins in the products of ZSM-5 supported catalysts is higher than that of MCM-41 supported catalysts.

Although quite a few satisfactory results have been achieved in the study of iron-based catalysts for ethylene selective oligomerization, however, the following aspects need to be improved. The co-catalyst MAO, which is used in iron-based catalysts for ethylene oligomerization, has brilliant catalytic effects while the cost of it is rather high. Therefor, exploring a new cheap and environment-friendly co-catalyst to replace MAO becomes necessary. And the use of molecular sieve carrier as a supported oligomerization catalyst can effectively improve the selectivity of oligomerization products, is also very helpful to maintain the thermal stability of the catalyst, while at the same time the activity of the catalyst system will be highly affected. Hence, exploring or synthesizing a carrier and a loading process which can maintain the activity of the catalyst system and even improve the activity of it is justified. Moreover, the activity and selectivity of iron-based catalysts for ethylene oligomerization are quite high while most iron-based catalysts are limited to ethylene dimerization only, further research is thus needed in the field of selective oligomerization of ethylene to produce high carbon α-olefin. Simply put, in-depth research can be carried out from the aspects of catalytic reaction mechanism, design and synthesis of ligands with new structures, *etc.* thus making the iron-based catalysts more favorable for ethylene selective oligomerization.

Conflicts of interest

Authors declare no competing interest.

Acknowledgements

This work was supported by the National Natural Science Foundation of China 51534004, U1362110 and Heilongjiang Touyan Innovation Team Program.

References

1 Z. Mohamadnia, L. Azimnavahsi and M. Soheili, *Polym. Sci., Ser. B*, 2018, **60**(2), 172–181.
2 Y. Ren, Y. Shi, X. Yao, *et al.*, *Polymers*, 2019, **11**(3), 434.

3 R. M. Swanepoel and C. E. Schwarz, *J. Chem. Eng. Data*, 2019, **64**(8), 3416–3435.
4 A. Gollwitzer, T. Dietel, W. P. Kretschmer, *et al.*, *Nat. Commun.*, 2017, **8**(1), 1226.
5 G. J. P. B. Dr, S. A. C. Dr, V. C. G. Prof, *et al.*, *Angew. Chem., Int. Ed.*, 2002, **41**(3), 489–491.
6 M. Soheili, Z. Mohamadnia and B. Karimi, *Catal. Lett.*, 2018, **148**(12), 3685–3700.
7 F. A. Alsherehy, *Stud. Surf. Sci. Catal.*, 1996, **100**, 515–523.
8 G. J. P. Britovsek, R. Malinowski, D. S. Mcguinness, *et al.*, *ACS Catal.*, 2015, **5**(11), 6922–6925.
9 Z. Xu, D. Zhao, D. J. P. Cha, *et al.*, *J. Catal*, 2017, **354**, 213–222.
10 D. S. Mcguinness, *Chem. Rev.*, 2011, **111**(3), 2321–2341.
11 Y. Yang, Z. Liu, L. Zhong, *et al.*, *Organometallics*, 2011, **30**(19), 5297–5302.
12 S. Härzschel, F. E. Kühn, A. Wöhl, *et al.*, *Catal.: Sci. Technol.*, 2015, **5**(3), 1678–1682.
13 Y. Kim, H. B. Im, U. H. Jung, *et al.*, *Fuel*, 2019, **256**, 115957.
14 H. Lee and S. H. Hong, *Appl. Catal., A*, 2018, **560**, 21–27.
15 J. Wang, Y. Li, C. Q. Li, *et al.*, *Chem. Eng. Prog.*, 2012, **31**(1), 91–97.
16 J. Wang, Z. J. Fu, C. Q. Li, *et al.*, *Polym. Mater. Sci. Eng.*, 2016, **7**, 176–183.
17 J. Wang, X. Y. Gong, C. Q. Li, *et al.*, *Chem. Eng. Prog.*, 2012, **31**(12), 2729–2735.
18 L. J. Yang, W. Z. Wang and Y. Wu, *Chin. J. Chem.*, 2014, **77**(10), 951–960.
19 C. Q. Li, Z. Y. Lin, J. Wang, *et al.*, *Synthetic Chemistry*, 2015, **23**(3), 198–201.
20 N. Savjani, K. Singh, *et al.*, *Inorg. Chim. Acta*, 2015, **436**, 184–194.
21 T. P. F. Xiao, W. J. Zhang, *et al.*, *C. R. Chim.*, 2011, **14**(9), 851–855.
22 C. Bianchini, G. Mantovani, A. Meli, *et al.*, *Eur. J. Inorg. Chem.*, 2003, **2003**(8), 1620–1631.
23 C. Gorl, N. Beck, K. Kleiber, *et al.*, *J. Mol. Catal.*, 2012, **352**, 110–127.
24 V. K. Appukuttan, Y. Liu, B. C. Son, *et al.*, *Organometallics*, 2011, **30**(8), 2285–2294.
25 C. Gorl and H. G. Alt, *J. Organomet. Chem.*, 2007, **692**(21), 4580–4592.
26 I. S. Maksakovaa, I. G. Pervovaa, I. N. Lipunova, *et al.*, *Petrochem*, 2015, **55**(3), 217–223.
27 J. Ma, C. Feng, S. L. Wang, *et al.*, *Inorg. Chem. Front.*, 2014, **1**(1), 14–34.
28 B. Burcher, P. A. R. Breuil, L. Magna, *et al.*, *Top. Organomet. Chem.*, 2015, **101**, 217–257.
29 S. Y. Jie, W. H. Sun and T. Xiao, *Chin. J. Polym. Sci.*, 2010, **28**(003), 299–304.
30 Y. Chen, R. Chen, C. Qian, *et al.*, *Organometallics*, 2003, **22**(21), 4312–4321.
31 W. H. Sun, S. Jie, S. Zhang, *et al.*, *Organometallics*, 2006, **25**(3), 666–677.
32 H. Wang, W. Dong, *et al.*, *Chin. Chem. Lett.*, 2003, **14**(3), 257–258.
33 N. Zhang, L. Chen, C. Li, *et al.*, *Russ. J. Phys. Chem.*, 2020, **94**, 1024–1033.
34 J. Wang, Y. T. Shang, *et al.*, *Russ. J. Phys. Chem. A*, 2018, **92**(13), 2618–2627.
35 M. Zhang, W. Zhang, T. Xiao, *et al.*, *J. Mol. Catal.*, 2010, **320**(1–2), 92–96.
36 H. Wang, *Chin. Sci. Bull.*, 2002, **47**(19), 1616–1618.
37 C. Li, D. Li, F. Wang, *et al.*, *Appl. Organomet. Chem.*, 2020, e5904.
38 S. Jie, S. Zhang, W. H. Sun, *et al.*, *J. Mol. Catal. A: Chem.*, 2007, **269**(1–2), 85–96.
39 J. Wang, J. Liu and L. Chen, *Transition Met. Chem.*, 2019, **44**(7), 681–688.
40 G. Xie, T. Li and A. Zhang, *Inorg. Chem. Commun.*, 2010, **13**(10), 1199–1202.
41 A. K. Tomov, V. C. Gibson, G. J. P. Britovsek, *et al.*, *Organometallics*, 2009, **28**(24), 7033–7040.
42 B. L. Small, R. Rios, E. R. Fernandez, *et al.*, *Organometallics*, 2010, **29**(24), 6723–6731.
43 A. Boudier, P. A. R. Breuil, L. Magna, *et al.*, *Chem. Commun.*, 2014, **50**(12), 1398–1407.
44 J. Ye, B. B. Jiang, *et al.*, *RSC Adv.*, 2015, **5**(116), 95981–95993.
45 W. Zhang, Cocatalyst optimization and its influence on iron-catalyzed ethylene oligomerization, Doctoral dissertation, Zhejiang University, 2018.
46 S. Moussa, N. P. Concepci, M. A. Arribas, *et al.*, *ACS Catal.*, 2018, **8**(5), 3903–3912.
47 O. L. Sydora, *Organometallics*, 2019, **38**(5), 997–1010.
48 S. J. Martinez, J. Ramos, V. Cruz, *et al.*, *Ameri. Chem. Soc.*, 2008, **112**(13), 5023–5028.
49 R. Raucoules, B. T. De, P. Raybaud, *et al.*, *Organometallics*, 2008, **27**(14), 3368–3377.
50 V. C. L. Cruz, J. Ramos, J. Martínez-Salazar, *et al.*, *Organometallics*, 2009, **28**(20), 5889–5895.
51 L. Chen, L. Ma, Y. Jiang, *et al.*, *Polym. Bull.*, 2020, 1–18.
52 V. C. Gibson, C. Redshaw and G. A. Solan, *Chem. Rev.*, 2007, **107**(5), 1745–1776.
53 B. L. Small and M. Brookhart, *J. Am. Chem. Soc.*, 1998, **120**(28), 7143–7144.
54 V. C. Gibson and S. K. Spitzmesser, *Chem. Rev.*, 2003, **103**(1), 283–316.
55 S. Mecking, *J. Cheminf.*, 2010, **32**(18), 534–540.
56 M. Wang, M. X. Qian and H. Ren, *Prog. Chem.*, 2001, **13**(2), 102–107.
57 W. H. Sun, P. Hao, S. Zhang, *et al.*, *Organometallics*, 2007, **26**(10), 2720–2734.
58 L. Xiao, R. Gao, M. Zhang, *et al.*, *Organometallics*, 2009, **28**(7), 2225–2233.
59 W. Yang, Z. Ma and W. H. Sun, *RSC Adv.*, 2016, **6**(83), 79335–79342.
60 C. Bianchini, G. Giambastiani, I. G. Rios, *et al.*, *Coord. Chem. Rev.*, 2006, **250**(11/12), 1391–1418.
61 M. Zhang, P. Hao, W. Zuo, *et al.*, *J. Organomet. Chem.*, 2008, **693**(3), 483–491.
62 M. Zhang, R. Gao, X. Hao, *et al.*, *J. Organomet. Chem.*, 2008, **693**(26), 3867–3877.

63 B. A. Schaefer, G. W. Margulieux, M. A. Tiedemann, *et al.*, Synthesis and Electronic Structure of Iron Borate Betaine Complexes as a Route to Single-Component Iron Ethylene Oligomerization and Polymerization Catalysts, *Organometallics*, 2015, **34**(23), 5615–5623.
64 W. Yang, Z. Ma, J. Yi, *et al.*, *Catalysts*, 2017, **7**(12), 120.
65 C. Bianchini, G. Giambastiani, I. G. Rios, *et al.*, *Organometallics*, 2007, **26**(20), 5066–5078.
66 W. H. Sun, Q. Xing, J. Yu, *et al.*, *Organometallics*, 2013, **32**(8), 2309–2318.
67 Z. Wang, G. A. Solan, W. Zhang, *et al.*, *Coord. Chem. Rev.*, 2018, **363**, 92–108.
68 W. Zhang, W. H. Sun and C. Redshaw, *Dalton Trans.*, 2013, **42**(25), 8988–8997.
69 M. F. Zheng, *Mater. Sci. Forum*, 2016, **859**, 158–161.
70 A. Boudier, P. A. R. Breuil, L. Magna, *et al.*, Novel catalytic system for ethylene oligomerization: an iron(III) complex with an anionic N,N,N ligand, *Organometallics*, 2011, **30**(10), 2640–2642.
71 W. H. Sun, S. Zhang and W. Zuo, *C. R. Chim.*, 2008, **11**(3), 307–316.
72 G. S. Nyamato, M. G. Alam, S. O. Ojwach, *et al.*, *J. Org. Chem.*, 2015, **783**, 64–72.
73 C. Q. Li, F. F. Wang, R. Gao, *et al.*, *Transition Met. Chem.*, 2017, **42**(4), 339–346.
74 M. Yankey, C. Obuah, I. A. Guzei, *et al.*, *Dalton Trans.*, 2014, **43**(37), 13913–13923.
75 N. Zhang, S. Wang, L. Song, *et al.*, *Inorg. Chim. Acta*, 2016, **453**, 369–375.
76 M. Haghverdi, A. Tadjarodi, N. Bahri-Laleh, *et al.*, *J. Coord. Chem.*, 2018, **71**(8), 1180–1192.
77 B. Li, X. Zhou, X. Liu, *et al.*, *Chem.–Asian J.*, 2019, **14**(9), 1582–1589.
78 T. Kondo, K. Yamamoto, T. Sakuragi, *et al.*, *Chem. Lett.*, 2012, **41**(4), 461–463.
79 L. Chen, M. J. Luo, F. Zhu, *et al.*, *J. Am. Chem. Soc.*, 2019, **141**(13), 5159–5163.
80 H. H. Zhang, J. J. Zhao and S. Yu, *J. Am. Chem. Soc.*, 2018, **140**(49), 16914–16919.
81 S. O. Ojwach, J. Darkwa., *Catal.: Sci. Technol.*, 2019, **9**(9), 2078–2096.
82 N. Zhang, J. Wang, H. Huo, *et al.*, *Inorg. Chim. Acta*, 2017, **469**, 209–216.
83 R. J. Trovitch, E. Lobkovsky and P. J. Chirik, *J. Am. Chem. Soc.*, 2008, **130**(35), 11631–11640.
84 S. Mctavish, G. J. P. Britovsek, T. M. Smit, *et al.*, *J. Mol. Catal.*, 2007, **261**(2), 293–300.
85 T. Suzuki, Y. Kajita and H. Masuda, *Dalton Trans.*, 2014, **43**(25), 9732–9739.
86 T. Zell, R. Langer, M. A. Iron, *et al.*, *Inorg. Chem.*, 2013, **52**(16), 9636–9649.
87 X. Xu, F. Luo, G. Zhou, *et al.*, *J. Mater. Chem. A*, 2018, **6**(38), 18396–18402.
88 Y. Song, D. Kim, H. J. Lee, *et al.*, *Inorg. Chem. Commun.*, 2014, **45**, 66–70.
89 C. Liu, Transition metal catalyzed cross-couplings of activated alkyl halides, Doctoral dissertation, Wuhan University, 2012.
90 B. W. Yu, L. B. Wang, T. T. Xu, H. L. Huo, *et al.*, *Spec. Petrochem.*, 2017, **34**(5), 78–82.
91 Y. Han, Y. Zhang, Y. Zhang, *et al.*, *Appl. Catal., A*, 2018, **564**, 183–189.
92 G. S. Nyamato, S. O. Ojwach and M. P. Akerman, *J. Mol. Catal.*, 2014, **394**, 274–282.
93 H. Sugiyama, G. Aharonian, S. Gambarotta, *et al.*, *J. Am. Chem. Soc.*, 2002, **124**(41), 12268–12274.
94 B. P. Carrow and L. Wang, *ACS Catal.*, 2019, **9**(8), 6821–6836.
95 W. Zhang, J. Ye, B. Jiang, *et al.*, *Can. J. Chem. Eng.*, 2018, **97**(4), 903–910.
96 S. Ramakrishnan and E. D. Jemmis, *J. Org. Chem.*, 2018, **865**, 37–44.
97 T. Li, M. Zheng, J. Liu, *et al.*, Catalyst composition and process for ethylene oligomerization, *US Pat.* 9266983, 2016-pp. 2–23.
98 A. Kermagoret, F. Tomicki and P. Braunstein, *Dalton Trans.*, 2008, **22**, 2945–2955.
99 Z. Boudene, A. Boudier, P. A. R. Breuil, *et al.*, *J. Catal*, 2014, **317**, 153–157.
100 K. P. Tellmann, V. C. Gibson, A. J. P. White, *et al.*, *Organometallics*, 2005, **24**(2), 280–286.
101 C. Gorl and H. G. Alt, *J. Mol. Catal.*, 2007, **273**(1–2), 118–132.
102 J. Wang, W. Li, B. Jiang, *et al.*, *J. Appl. Polym. Sci.*, 2010, **113**(4), 2378–2391.
103 Y. J. Chen, P. Hao, *et al.*, *J. Organomet. Chem.*, 2008, **693**(10), 1829–1840.
104 L. P. Zhang, X. H. Hou, *et al.*, *Inorg. Chim. Acta*, 2011, **379**(1), 70–75.
105 J. Ye, Mediating the micro-chemical environment of the active species in iron catalysts and its application in ethylene oligomerization, Doctoral dissertation, Zhejiang University, 2015.
106 W. Zhang, B. B. Jiang, J. Ye, *et al.*, *Chin. J. Polym. Sci.*, 2018, **36**(11), 1207–1216.
107 Y. C. Qin, Exploring the Modulating Effects of Phenolic Modifiers on Ethylene Oligomerization Catalyzed by Transition Metal Catalyst, Master dissertation, Zhejiang University, 2016.
108 R. Steiger, *Polyhedron*, 1988, **7**(22), 2375–2381.
109 L. D. Li, Influences of Activators on Ethylene Polymerization Catalyzed by Iron Complexes and Synthesis of Polyethylene with Broad/Bimodal Molecular Weight Distribution, Doctoral dissertation, Zhejiang University, 2005.
110 M. J. Hanton and K. Tenza, *Organometallics*, 2010, **27**(21), 5712–5716.
111 M. E. Z. Velthoen and A. Muñoz-Murillo, *Macromolecules*, 2018, **51**(2), 343–355.
112 T. Ryo, K. Tomoyasu, S. Yuto, *et al.*, *Macromolecules*, 2017, **50**(15), 5989–5993.
113 L. Mikko, C. Scott, *et al.*, *ChemPhysChem*, 2017, **18**(23), 3288.

114 I. S. Pavlova, I. G. Pervova, G. P. Belov, *et al.*, *Pet. Chem.*, 2013, **53**(2), 127–133.
115 M. X. Qian, M. Wang, *et al.*, *J. Mol. Catal.*, 2000, **160**(2), 243–247.
116 A. F. R. Kilpatrick, N. H. Rees, S. Sripothongnak, *et al.*, *Organometallics*, 2017, **37**(1), 156–164.
117 P. A. R. Breuil, L. Magna and B. H. Olivier, *Dalton Trans.*, 2015, **44**(29), 12995–12998.
118 J. Ye, Y. Li, B. Jiang, *et al.*, *Polym. Eng. Sci.*, 2019, **59**(5), 1010–1016.
119 L. B. Small, *Acc. Chem. Res.*, 2015, **48**(9), 150812155019009.
120 G. J. Britovsek, S. Mastroianni, G. A. Solan, *et al.*, *Chemistry*, 2015, **6**(12), 2221–2231.
121 Y. Chen, C. Qian and J. Sun, *Organometallics*, 2003, **22**(6), 1231–1236.
122 C. M Ángeles, G. D. A. Rodr, P. Palma, *et al.*, *Catal.: Sci. Technol.*, 2014, **4**(8), 2504–2507.
123 D. Thiele and R. F. D. Souza, Oligomerization of Ethylene Catalyzed by Iron and Cobalt in Organoaluminate Dialkylimidazolium Ionic Liquids, *Catal. Lett.*, 2010, **138**(1–2), 50–55.
124 P. Kumkaew, S. E. Wanke, P. Praserthdam, *et al.*, *J. Appl. Polym. Sci.*, 2003, **87**(7), 1161–1177.
125 C. Huang, K. G. Neoh, L. Xu, *et al.*, *Biomacromolecules*, 2012, **13**(8), 2513–2520.
126 S. Paenkaew, T. Kajornprai and M. Rutnakornpituk, *Polym. Adv. Technol.*, 2020, 31.
127 W. Injumpa, P. Ritprajak and N. Insin, *J. Magn. Magn. Mater.*, 2016, **427**, 60–66.
128 S. Ghosh, S. Ghoshmitra, T. Cai, *et al.*, *Nanoscale Res. Lett.*, 2009, **5**(1), 195–204.
129 P. Kumkaew, L. Wu, P. Praserthdam, *et al.*, *Polymer*, 2003, **44**(17), 4791–4803.
130 X. Wang, C. Zhang, W. Liu, *et al.*, *Polymers*, 2018, **10**(9), 944.
131 A. Kurek, R. Xalter, M. Stürzel, *et al.*, *Macromolecules*, 2013, **46**(23), 9197–9201.
132 J. N. Kuhn, W. Huang, C. K. Tsung, *et al.*, *J. Am. Chem. Soc.*, 2008, **130**(43), 14026–14027.
133 M. Davidson, C. Ngo, S. H. Gage, *et al.*, *Microporous Mesoporous Mater.*, 2019, **276**, 270–279.
134 C. Y. Guo, H. Xu, M. Zhang, *et al.*, *Polym. Int.*, 2010, **59**(6), 725–732.
135 C. Y. Guo, H. Xu, M. Zhang, *et al.*, *Catal. Commun.*, 2009, **10**(10), 1467–1471.
136 M. Zhang, H. Xu, C. Guo, *et al.*, *Polym. Int.*, 2005, **54**(2), 274–278.
137 J. Arumugam, G. S. Nyamato and S. O. Ojwach, *J. Org. Chem.*, 2009, **903**, 120987.
138 H. Yao, S. Hu, Y. Wu, *et al.*, *Pol. J. Environ. Stud.*, 2019, **28**(4), 2491–2499.
139 J. Ye, L. Gagliardi, C. J. Cramer, *et al.*, *J. Catal*, 2018, **360**, 160–167.
140 M. H. Firouzjaee and M. Taghizadeh, *Chem. Eng. Technol.*, 2017, **40**(6), 1140–1148.
141 K. P. Thanh, R. Paola, B. Guido, *et al.*, *Fuel Process. Technol.*, 2015, **137**, 290–297.
142 H. G. H. Ricardo, C. C. H. Juan, O. P. Quintana, *et al.*, *Top. Cat.*, 2020, **63**(5–6), 414–427.
143 J. Canivet, S. Aguado, Y. Schuurman, *et al.*, *J. Am. Chem. Soc.*, 2013, **135**(11), 4195–4198.
144 H. Xu and C. Y. Guo, *Eur. Polym. J.*, 2015, **65**, 15–32.
145 Q. Chen, H. Suo, W. Zhang, *et al.*, *Dalton Trans.*, 2019, **48**(21), 8264–8278.
146 M. E. Bluhm, C. Folli and M. DöRing, *J. Mol. Catal.*, 2004, **212**(1–2), 13–18.
147 Z. Ma, W. H. Sun, Z. L. Li, *et al.*, *Polym. Int.*, 2002, **51**(10), 994–997.
148 A. Behr, N. Rentmeister and D. MöLler, *Catal. Commun.*, 2014, **55**, 38–42.
149 J. Ye, B. Jiang, J. Wang, *et al.*, *J. Polym. Sci., Part A: Polym. Chem.*, 2015, **52**(19), 2748–2759.
150 S. S. Karpiniec, D. S. Mcguinness, G. J. P. Britovsek, *et al.*, *Organometallics*, 2012, **31**(8), 3439–3442.

